

PeptideScience

THE AMERICAN PEPTIDE SOCIETY JOURNAL

Special Issue: Peptide Engineering Meeting 8

Guest Editors: Prof. Beate Kokschi (Freie Universität Berlin), Dr Joel P. Schneider (National Institutes of Health), Prof. Peter H. Seeberger (Max Planck Institute of Colloids and Interfaces) and Prof. Claudio Toniolo (University of Padova)

EDITORIALS

Peptide Engineering Meeting 8

Beate Kokschi and Peter H. Seeberger, *Peptide Science* 2020, doi: [10.1002/pep2.24146](https://doi.org/10.1002/pep2.24146)

Peptide Engineering Meetings (PEMs): Evolution from PEM6 to PEM8

Claudio Toniolo, *Peptide Science* 2020, doi: [10.1002/pep2.24131](https://doi.org/10.1002/pep2.24131)

REVIEWS

Bent into shape: Folded peptides to mimic protein structure and modulate protein function

Haley I. Merrit, Nicholas Sawyer and Paramjit S. Arora, *Peptide Science* 2020, doi:

[10.1002/pep2.24145](https://doi.org/10.1002/pep2.24145)

Helical polysaccharides

Varsha J. Thombare and Craig A. Hutton, *Peptide Science* 2020, doi: [10.1002/pep2.24124](https://doi.org/10.1002/pep2.24124)

FULL PAPERS

Influence of the C-terminal substituent on the crystal-state conformation of Adm peptides

Fatemeh M. Mir, Marco Crisma, Claudio Toniolo and William D. Lubell, *Peptide Science* 2020, doi: [10.1002/pep2.24121](https://doi.org/10.1002/pep2.24121)

Halogen bonding as a key interaction in the self-assembly of iodinated diphenylalanine peptides

Andrea Pizzi, Luca Catalano, Nicola Demitri, Valentina Dichiarante, Giancarlo Terraneo and Pierangelo Metrangolo, *Peptide Science* 2020, doi: [10.1002/pep2.24127](https://doi.org/10.1002/pep2.24127)

Redox degradable 3-elix micelles with tunable sensitivity

Yi Xue, Benson T. Jung and Ting Xu, *Peptide Science* 2020, doi: [10.1002/pep2.24117](https://doi.org/10.1002/pep2.24117)

Instructed-assembly of small peptides inhibits drug-resistant prostate cancer cells

Zhaogiangi Feng, Huaimin Wang, Meihui Yi, Chieh-Yun Lo, Ashanti Sallee, Jer-Tsong Hsieh and Bing Xu, *Peptide Science* 2020, doi: [10.1002/pep2.24123](https://doi.org/10.1002/pep2.24123)

Induced α,γ -cyclic peptide rotodimer recognition by nucleobase scaffolds

Michele Panciera, Eva González-Freire, Martin Calvelo, Manuel Amorín and Juan R. Granja, *Peptide Science* 2020, doi: [10.1002/pep2.24132](https://doi.org/10.1002/pep2.24132)

Short self-assembling cationic antimicrobial peptide mimetics based on a 3,5-diaminobenzoic acid scaffold

Chaitanya K. Thota, Allison A. Berger, Björn Harms, Maria Seidel, Christoph Böttcher, Hans von Berlepsch, Chaunxiong Xie, Roderich Süßmuth, Christian Roth and Beate Kokschi, *Peptide Science* 2020, doi: [10.1002/pep2.24130](https://doi.org/10.1002/pep2.24130)

The effect of turn residues on the folding and cell-penetrating activity of β -hairpin peptides and applications toward protein delivery

Stephen E. Miller and Joel P. Schneider, *Peptide Science* 2020, doi: [10.1002/pep2.24125](https://doi.org/10.1002/pep2.24125)



PeptideScience

THE AMERICAN PEPTIDE SOCIETY JOURNAL

Special Issue: Peptide Engineering Meeting 8

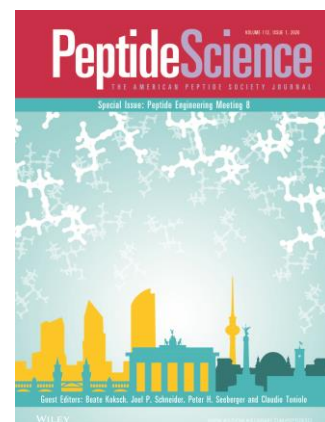
Guest Editors: Prof. Beate Koksich (Freie Universität Berlin), Dr Joel P. Schneider (National Institutes of Health), Prof. Peter H. Seeberger (Max Planck Institute of Colloids and Interfaces) and Prof. Claudio Toniolo (University of Padova)

Conversion of cationic amphiphilic lytic peptides to cell-penetration peptides

Hao-Hsin Yu, Kentarou Sakamoto, Misao Akishiba, Naoki Tamemoto, Hisaaki Hirose, Ikuhiko Nakase, Miki Imanishi, Fatemeh Madani, Astrid Gräslund and Shiroh Futaki, *Peptide Science* 2020, doi: [10.1002/pep2.24144](https://doi.org/10.1002/pep2.24144)




Spiegelmeric 4RIS-hydroxy/amino-L/D-prolyl collagen peptides: Conformation and morphology of self-assembled structures

Shahaji H. More and Krishna N. Ganesh, *Peptide Science* 2020, doi: [10.1002/pep2.24140](https://doi.org/10.1002/pep2.24140)



FULL PAPER

Instructed-assembly of small peptides inhibits drug-resistant prostate cancer cells

Zhaoqianqi Feng¹  | Huaimin Wang¹  | Meihui Yi¹ | Chieh-Yun Lo¹ |
Ashanti Sallee¹ | Jer-Tsong Hsieh² | Bing Xu¹ 

¹Department of Chemistry, Brandeis University, 415 South Street, Waltham, Massachusetts

²Department of Urology, Southwestern Medical Center, University of Texas, Dallas, Texas

Correspondence

Bing Xu, Department of Chemistry, Brandeis University, 415 South Street, Waltham, MA 02454.

Email: bxu@brandeis.edu

Funding information

National Institutes of Health, Grant/Award Numbers: F99CA234746, R01CA142746; National Science Foundation, Grant/Award Number: DMR-1420382

Abstract

Despite multiple new-drug approvals in recent years, prostate cancer remains a global health challenge because of the prostate cancers are resistant to androgen deprivation therapy. Here, we show that a small D-phosphopeptide undergoes prostatic acid phosphatase (PAP)-instructed self-assembly for inhibiting castration-resistant prostate cancer (CRPC) cells. Specifically, the installation of phosphate at the C-terminal of a D-tripeptide results in the D-phosphopeptide. Dephosphorylating the D-phosphopeptide by PAP forms uniform nanofibers that inhibit VCaP, a CRPC cell. A non-hydrolyzable phosphate analogue of the D-phosphopeptide, which shares similar self-assembling properties with the D-phosphopeptide, confirms that PAP-instructed assembly is critical for the inhibition of VCaP. This work, for the first time, demonstrates PAP-instructed self-assembly of peptides for selective inhibiting CRPC cells.

KEYWORDS

drug resistance, enzyme, prostate cancer, self-assembly, selective inhibition

1 | INTRODUCTION

Prostate cancer is the most frequent cancer and the second leading cause of cancer death among males in United States.^[1] Although the initial treatment of prostate cancer—surgery or radiation therapy—could cure patients with localized tumors, the cancer recurs and spreads to other organs, such as bone. Androgen deprivation therapy, the mainstay of therapy, is effective for treating recurrent prostate cancer in early stage, because the tumor growth is initially androgen dependent.^[2] However, the development of castration-resistant prostate cancer (CRPC)^[3] causes tumor regression and resistance against androgen ablation. Despite the intensive treatments, the 5-year survival rate of patients with CRPC is only approximately 30%.^[4] Therefore, it is necessary to develop new approaches for treating CRPC.

Enzyme-instructed self-assembly (EISA), a prevalent phenomenon in nature, is emerging as a new approach, which is fundamentally different from ligand-receptor interactions, for controlling cell fates. In fact, EISA of small molecules (e.g., peptides,^[5] sterols,^[6] saccharides,^[7] and lipids^[8]) generating supramolecular assemblies in

situ is being actively explored for potential cancer therapy. Our previous studies show that supramolecular assemblies formed through EISA selectively inhibit tumor cells via multiple mechanisms^[9] without causing acquired drug resistance.^[10] Moreover, the precise spatiotemporal control of EISA enables the selective targeting of the loss-of-function^[11] and subcellular organelles (e.g., mitochondria,^[10,12] endoplasmic reticulum,^[13] and plasma membrane^[12]) in cancer cells. Several other laboratories also have validated this approach for cancer therapy in cell assays and in animal models. For example, Maruyama *et al.* demonstrated that matrix metalloproteinase-7 triggered the intracellular EISA of a lipid-peptide conjugate to induce cancer cell (HeLa) death.^[8] A carbohydrate phosphate derivative, reported by Pires and Ulijn *et al.*, undergoes EISA to form nanofibers to selectively inhibit the metabolic activity of osteosarcoma (Saos-2) cells.^[7] Yang and coworkers used tandem molecular self-assembly in liver cancer cells for inhibiting cancer cells.^[14] Besides demonstrating therapeutic efficacies in various human tumors, supramolecular assemblies formed by EISA have also been applied in molecular imaging for cancer diagnosis. For example, Rao and coworkers first developed

enzyme triggered condensation reaction for imaging tumor in a murine model.^[15] Liang *et al.* used the EISA of gadolinium containing nanofibers to enhance T2 contrast for magnetic resonance imaging of tumor.^[16] Recently, Kuang *et al.* reported the use of EISA of peptides to selectively eliminate undifferentiated human induced pluripotent stem cells (iPSCs).^[17]

Based on these encouraging results, we chose to employ peptide derivatives as the building blocks for EISA to inhibit CRPC cells. Peptide assemblies are uniquely advantageous for biomedical applications because peptides exhibit good biocompatibility,^[18] undergo tunable degradation,^[19] are able to switch conformations,^[20–22] minimize immunogenicity,^[23,24] and fit well with available computational designing platforms.^[25] These unique properties already have fostered the increasing explorations of peptide assemblies for various biomedical applications.^[26–29]

Taking advantage of the elevated level of prostatic acid phosphatase (PAP) in patients with prostate cancer,^[30] we designed a peptidic precursor **1-EP**, as the substrate of PAP, to serve as the EISA precursor (Figure 1). Replacing the phosphate group in **1-EP** with phosphonate generates precursor **1-CP**, which resists PAP, as the control of **1-EP**. As revealed by transmission electron microscopy (TEM) and critical micelle concentration (CMC) test, **1-EP** and **1-CP** share similar self-assembling properties. Although PAP dephosphorylates **1-EP** into **1-E**, which self-assembles to form uniform nanofibers from short irregular nanoribbons, the treatment of PAP results in little change in the morphology of the nanostructures formed by **1-CP**. Moreover, **1-EP** potentially inhibits both androgen-dependent prostate cancer cells (LNCaP) and CRPC cells (VCaP), whereas **1-CP** exhibits little toxicity to those cells. These results validate that PAP-instructed assembly is critical for inhibiting prostate cancers and provide an alternative strategy for killing CRPC.

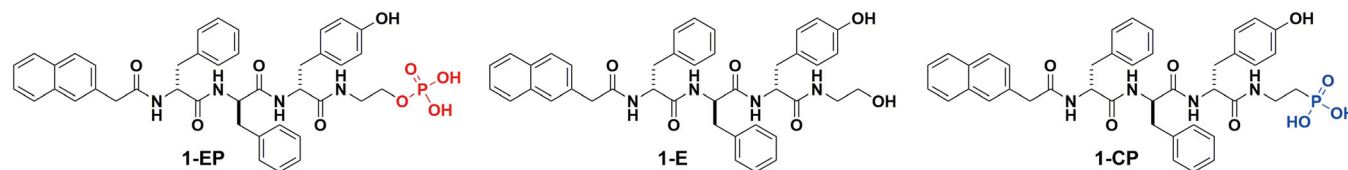


FIGURE 1 Molecular structures of **1-EP**, **1-E** and **1-CP**

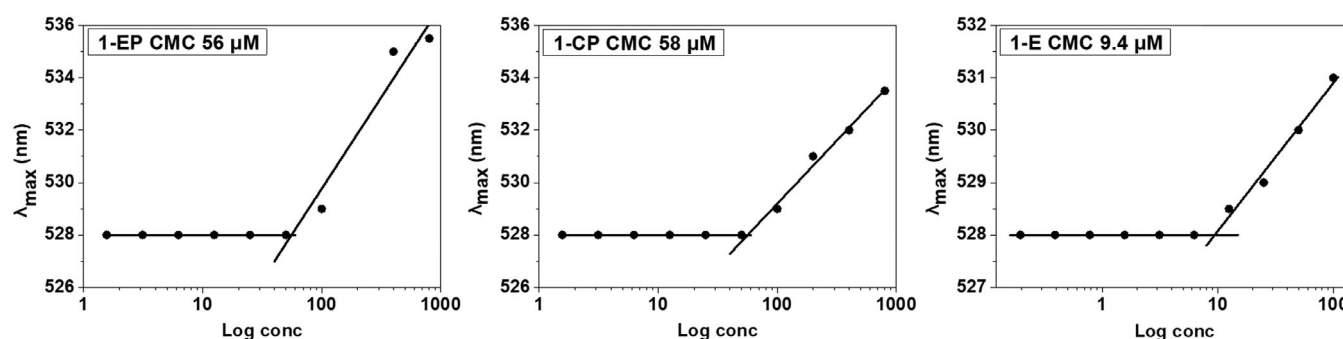


FIGURE 2 Critical micelle concentrations of **1-EP**, **1-CP**, and **1-E**

2 | MATERIALS AND METHODS

2.1 | Synthesis and characterization of precursors

2-Cl-trityl chloride resin (0.8–1.0 mmol/g), HBTU, and Fmoc-amino acids were purchased from GL Biochem (Shanghai, China). Other chemical reagents and solvents were obtained from Fisher Scientific. We synthesized peptide **1-EP**, **1-CP**, and **1-E** by combining solid phase peptide synthesis (SPPS) and solution-phase synthesis (Supporting Information Scheme S2). After the synthesis, all compounds were purified using a reverse phase HPLC (Agilent 1100 Series) with HPLC grade acetonitrile (0.1% TFA) and HPLC grade water (0.1% TFA) as the eluents. The ¹H-NMR and ³¹P-NMR spectra of compounds were obtained using Varian 400 MR and LC-MS spectra using a Waters Acquity Ultra Performance LC with Waters MICROMASS detector (Supporting Information Figures S1–8). The LC-MS eluents are LC-MS grade acetonitrile (0.1% formic acid) and LC-MS grade water (0.1% formic acid).

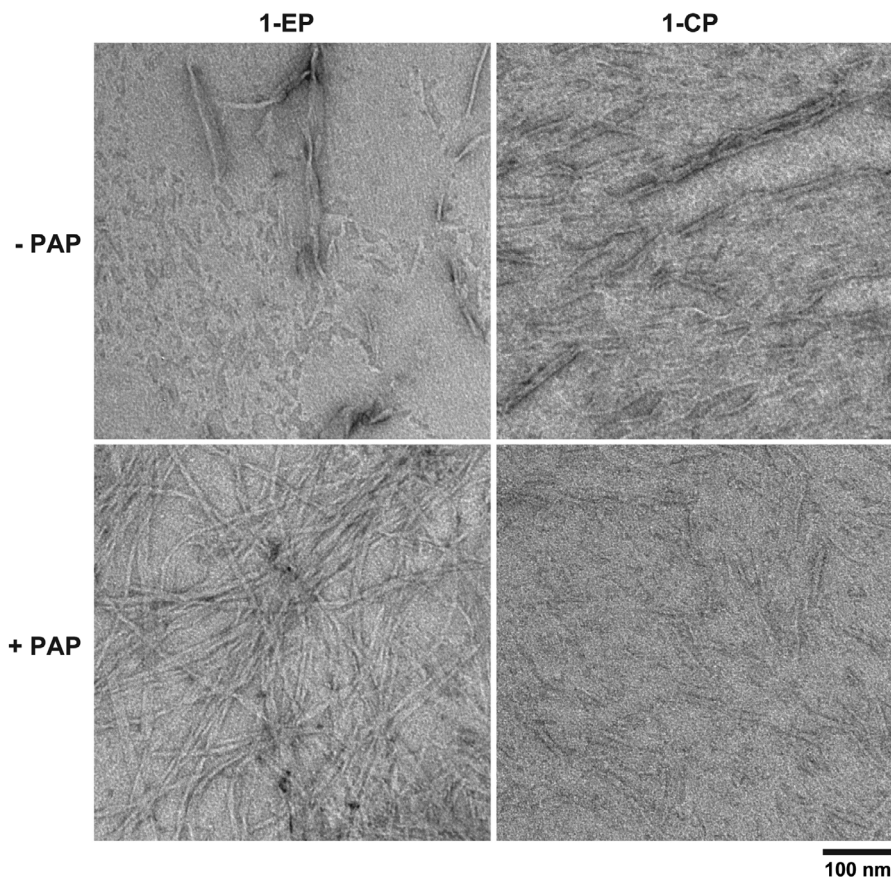
2.2 | CMC measurements

A series of solutions of **1-EP**, **1-CP**, or **1-E**, from the concentration of 800 μM to 1.6 μM, were prepared in pH 5.6 citrate-phosphate buffer. After incubating with 5 μM Rhodamine 6G, the absorbance from 520 to 540 nm were measured, using a Biotek Synergy multi-mode microplate reader, to determine the λ_{\max} for plotting.

2.3 | Transmission electron microscopy

Solution of **1-EP** (100 μM) and **1-CP** (100 μM) were prepared in pH 5.6 citrate-phosphate buffer, with or without the treatment of PAP (1 U/mL, 1 U = 1 μmol/min at pH 5.6 and 37 °C) for 24 hours.

FIGURE 3 TEM images of nanostructures formed before and after adding prostatic acid phosphatase (PAP) (1 U/ mL) to the solution of **1-EP** and **1-CP** (100 μ M) in pH 5.6 citrate-phosphate buffer for 24 hours. Scale bar = 100 nm



Placing 5 μ L samples on the glow discharged 400 mesh copper grids coated with continuous thick carbon film (SPI Supplies), we stained the sample loaded grid with the uranyl acetate and allowed the samples to dry in air for direct imaging. TEM images were obtained with Morgagni 268 transmission electron microscope.

2.4 | Cell culture

LNCaP and HS-5 cells were purchased from American Type Culture Collection (ATCC). VCaP cells were given by Dr. Jer-Tsong Hsieh lab. VCaP, and HS-5 cells were cultured in Dulbecco's Modified Eagle Medium (DMEM) supplemented with 10% v/v fetal bovine serum (FBS), LNCaP cells in RPMI 1640 Medium supplemented with 10% v/v FBS. All the culture mediums were supplemented with 100 U/mL penicillin and 100 μ g/mL streptomycin. And, the cells were maintained at 37 $^{\circ}$ C in a humidified atmosphere of 5% CO₂.

2.5 | MTT assay

The cell viability was determined by MTT assay. Cells were seeded in 96-well plates at 1×10^4 cells/well for 24 hours followed by culture medium removal and addition of culture medium containing different concentration of **1-EP** or **1-CP** (200 μ M, 100 μ M, 50 μ M, 20 μ M, 10 μ M). After 24/48/72 hours incubation, we added 10 μ L 3-(4,5-dimethylthiazol-2-yl)-2,5-diphenyltetrazolium bromide (MTT)

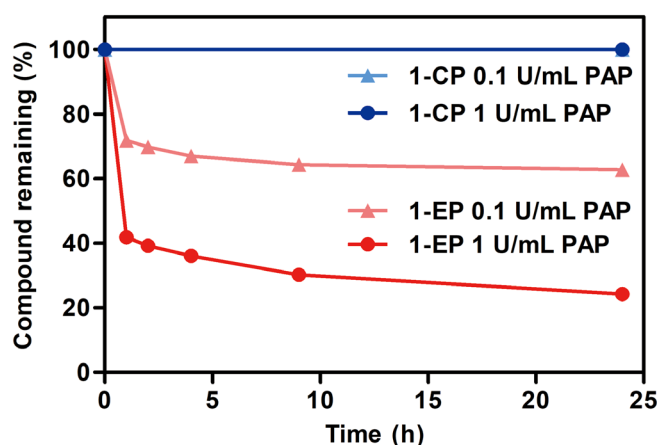


FIGURE 4 Dephosphorylation of **1-EP** and **1-CP** (200 μ M) after incubating with prostatic acid phosphatase (PAP) (1 U/ mL or 0.1 U/ mL) in pH 5.6 citrate-phosphate buffer

solution (5 mg/mL) to each well followed by incubating the plate at 37 $^{\circ}$ C for another 4 hours. One hundred microliters of SDS-HCl solution was added to stop the reduction reaction and to dissolve the formazan. After measuring the absorbance of each well at 595 nm with multimode microplate reader, we calculated the cell viability percentage relative to the untreated cells. The MTT assay was performed in triplicate, and the average value of the three measurements was taken.

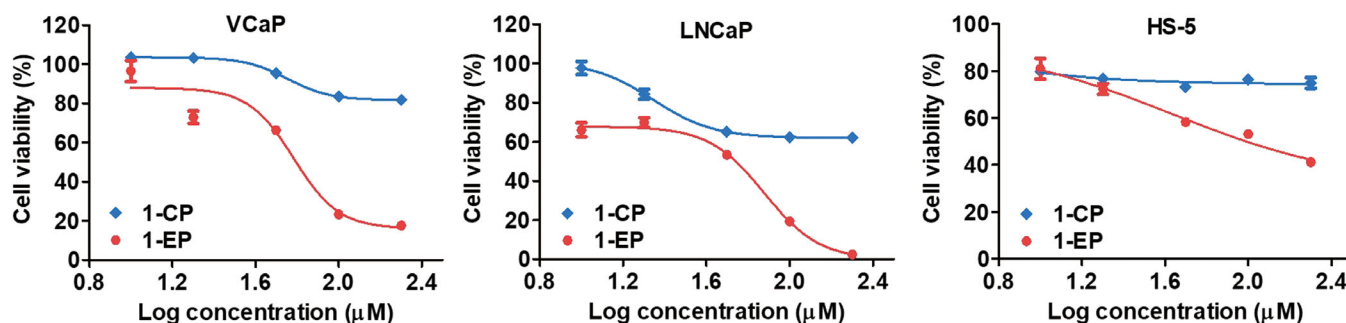


FIGURE 5 Cell viabilities of VCaP, LNCaP, and HS-5 cells after treating with 1-EP and 1-CP at the concentrations of 200 μM , 100 μM , 50 μM , 20 μM , 10 μM for 72 hours

3 | RESULTS AND DISCUSSION

3.1 | Molecular design

The precursor **1-EP** consists of a D-peptide backbone (D-Phe-D-Phe-D-Tyr) as the proteolytic resistant, self-assembling motif, a phosphorylethanolamine as a substrate of PAP, and an N-terminal capping group (2-naphthylacetyl) to enhance aromatic-aromatic interactions (Figure 1). Because of the PAP overexpression in prostate cancer,^[30] including CRPC, such a design allows **1-EP** to undergo EISA in prostate cancer cells to inhibit prostate cancer cells regardless of their sensitivities against androgen deprivation. To validate the importance of EISA process, we designed a nonhydrolytic analogue, **1-CP**, by replacing the phosphate group in **1-EP** with phosphonate.

3.2 | Self-assembly *in vitro*

After synthesizing and purifying the precursors, we first evaluated their self-assembling ability by measuring the CMC of the precursors, using Rhodamine 6G as a probe. Although the CMC of **1-EP** is 56 μM , its dephosphorylated product **1-E** exhibit a CMC of 9.4 μM (Figure 2), suggesting that the dephosphorylation of **1-EP** increases the self-assembling ability of the resulting molecules. In addition, the comparable CMC values of **1-CP** (58 μM) and **1-EP** (56 μM) indicate that **1-EP** and **1-CP** have similar self-assembling abilities. The TEM images show that both **1-EP** and **1-CP** self-assemble to form irregular nanoribbon-like structures in the pH 5.6 citrate-phosphate buffer (Figure 3). The enzymatic activity of PAP is sensitive to pH, with optimum at pH 5.6;^[31] therefore, we chose this pH for *in vitro* experiments. Upon the treatment with PAP, **1-EP** turns into **1-E**, which self-assembles to form uniform nanofibers with a diameter of 6 ± 2 nm, validating the morphological transition resulted from EISA of **1-EP**. In contrast to the case of **1-EP**, **1-CP** exhibits little morphology change after treating with PAP, confirming that PAP is unable to trigger the EISA of **1-CP**.

3.3 | Enzyme-catalyzed molecular transformation

To investigate the kinetics of EISA process, we evaluated the time-dependent dephosphorylation of the precursors at different enzyme concentrations (i.e., 0.1 U/mL and 1 U/mL). Although 0.1 U/mL PAP

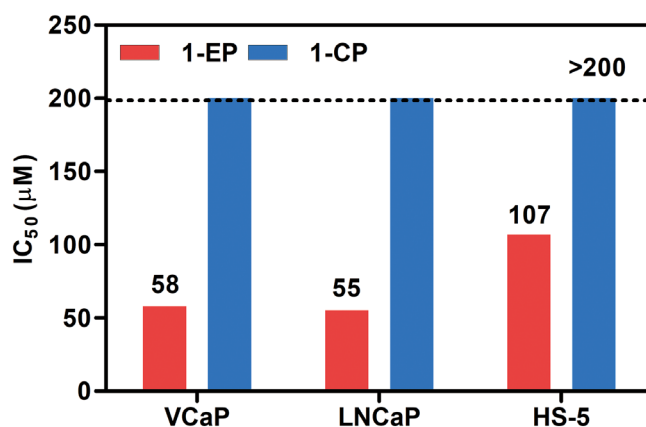


FIGURE 6 Summary of IC_{50} (72 hours) of 1-EP and 1-CP against VCaP, LNCaP, and HS-5 cells

converted 28%, 30%, 33%, 36%, 37% of **1-EP** to **1-E**, 1 U/mL PAP dephosphorylated 58%, 61%, 64%, 70%, 76% of **1-EP**, after 1 hour, 2 hours, 4 hours, 9 hours, 24 hours of incubation, respectively (Figure 4). These results reveal that the dephosphorylation rates of **1-EP** correspond to the concentrations of PAP, indicating that the PAP expression of cancer cells could kinetically control the EISA process.^[32] In addition, incubating **1-CP** with PAP hardly results in any conversion of **1-CP**, confirming that **1-CP** is unable to undergo PAP-instructed self-assembly.

3.4 | Inhibitory activities against different cell lines

We next examined the anticancer activity of the precursors against PAP expressing prostate cancer cells, including an androgen-sensitive prostate cancer cell line LNCaP^[33] and a CRPC cell line VCaP.^[34] As shown in Figure 5, **1-EP** inhibits both VCaP and LNCaP in a dose-dependent manner, with an IC_{50} of 58 and 55 μM , respectively (Figure 6), indicating that EISA of **1-EP** inhibits prostate cancer cells regardless of their androgen sensitivities. To evaluate the selectivity of **1-EP**, we also tested its toxicity on a normal stromal cell line HS-5 and found that **1-EP** exhibited less cytotoxicity to HS-5 cells with an IC_{50} of 107 μM , (Figure 6) although HS-5 is known to express acid phosphatase,^[35] likely due to the lower PAP expression in normal cells. In addition, we also tested the cytotoxicity of the precursors

against another prostate cancer cell line DU 145^[33] that express little PAP and found that 1-EP only inhibits DU 145 at 200 μ M (Supporting Information Figure S9). These results suggest that the PAP expression is important for the inhibition. In contrast to the case of **1-EP**, the IC₅₀ of **1-CP** on LNCaP and VCaP are both above 200 μ M, validating that EISA processes play critical roles in inhibiting prostate cancer.

4 | CONCLUSIONS

In conclusion, this study demonstrates the first example that the prostate cancer marker, PAP, is able to catalyze the self-assembly of peptides for selectively inhibiting CRPC. This strategy not only provides a potential alternative therapy for CRPC but also highlights the rationale of cancer markers instructed-assembly for tumor inhibition. Although the concentration of the precursor for inhibiting cancer cells currently appears higher than the normal dosage of conventional clinical drugs, the selectivity of the precursor warrants further exploration. For example, the precursor with high self-assembling ability^[32] would likely lower the dosage. Moreover, the use of non-hydrolyzable phosphate analogue undoubtedly confirms that EISA in/on cancer cells is the origin of tumor inhibition.

ACKNOWLEDGMENT

This work is partially supported by NIH (R01CA142746) and NSF (DMR-1420382). Z.F. is supported by NIH (F99CA234746).

ORCID

Zhaoqianqi Feng  <https://orcid.org/0000-0002-1262-385X>

Huaimin Wang  <https://orcid.org/0000-0002-8796-0367>

Bing Xu  <https://orcid.org/0000-0002-4639-387X>

REFERENCE

- [1] F. Bray, J. Ferlay, I. Soerjomataram, R. L. Siegel, L. A. Torre, A. Jemal, *Ca-Cancer J. Clin.* **2018**, 68, 394.
- [2] B. J. Feldman, D. Feldman, *Nat. Rev. Cancer* **2001**, 1, 34.
- [3] F. R. Ahmann, E. D. Crawford, W. Kreis, Y. Levasseur, *Cancer Res.* **1987**, 47, 4736.
- [4] C. Logothetis, M. J. Morris, R. Den, R. E. Coleman, *Cancer Metastasis Rev.* **2018**, 37, 189.
- [5] Z. M. Yang, K. M. Xu, Z. F. Guo, Z. H. Guo, B. Xu, *Adv. Mater.* **2007**, 19, 3152.
- [6] H. M. Wang, Z. Q. Q. Feng, D. D. Wu, K. J. Fritzsche, M. Rigney, J. Zhou, Y. J. Jiang, K. Schmidt-Rohr, B. Xu, *J. Am. Chem. Soc.* **2016**, 138, 10758.
- [7] R. A. Pires, Y. M. Abul-Haija, D. S. Costa, R. Novoa-Carballal, R. L. Reis, R. V. Ulijn, I. Pashkuleva, *J. Am. Chem. Soc.* **2015**, 137, 576.
- [8] A. Tanaka, Y. Fukuoka, Y. Morimoto, T. Honjo, D. Koda, M. Goto, T. Maruyama, *J. Am. Chem. Soc.* **2015**, 137, 770.
- [9] H. Wang, Z. Feng, C. Yang, J. Liu, J. E. Medina, S. A. Aghvami, D. M. Dinulescu, J. Liu, S. Fraden, B. Xu, *Mol. Cancer Res.* **2019**, 17, 907.

- [10] H. Wang, Z. Feng, Y. Wang, R. Zhou, Z. Yang, B. Xu, *J. Am. Chem. Soc.* **2016**, 138, 16046.
- [11] Z. Feng, H. Wang, R. Zhou, J. Li, B. Xu, *J. Am. Chem. Soc.* **2017**, 139, 3950.
- [12] H. He, J. Wang, H. Wang, N. Zhou, D. Yang, D. R. Green, B. Xu, *J. Am. Chem. Soc.* **2018**, 140, 1215.
- [13] Z. Feng, H. Wang, S. Wang, Q. Zhang, X. Zhang, A. A. Rodal, B. Xu, *J. Am. Chem. Soc.* **2018**, 140, 9566.
- [14] J. Zhan, Y. Cai, S. He, L. Wang, Z. Yang, *Ang. Chem. Int. Ed.* **2018**, 57, 1813.
- [15] G. Liang, H. Ren, J. Rao, *Nat. Chem.* **2010**, 2, 54.
- [16] L. Dong, J. Qian, Z. Hai, J. Xu, W. Du, K. Zhong, G. Liang, *Anal. Chem.* **2017**, 89, 6922.
- [17] Y. Kuang, K. Miki, C. J. C. Parr, K. Hayashi, I. Takei, J. Li, M. Iwasaki, M. Nakagawa, Y. Yoshida, H. Saito, *Cell Chem. Biol.* **2017**, 24, 685.
- [18] T. Aida, E. W. Meijer, S. I. Stupp, *Science* **2012**, 335, 813.
- [19] R. P. Cheng, S. H. Gellman, W. F. DeGrado, *Chem. Rev.* **2001**, 101, 3219.
- [20] J. F. Shi, G. Fichman, J. P. Schneider, *Ang. Chem., Int. Ed.* **2018**, 57, 11188.
- [21] D. F. Kreidler, Z. Yao, J. D. Steinkruger, D. E. Mortenson, L. Huang, R. Mittal, B. R. Travis, K. T. Forest, S. H. Gellman, *J. Am. Chem. Soc.* **2019**, 141, 1583.
- [22] E. G. Baker, G. J. Bartlett, K. L. P. Goff, D. N. Woolfson, *Acc. Chem. Res.* **2017**, 50, 2085.
- [23] A. W. Purcell, W. G. Zeng, N. A. Mifsud, L. K. Ely, W. A. MacDonald, D. C. Jackson, *J. Pept. Sci.* **2003**, 9, 255.
- [24] J. S. Rudra, Y. F. Tian, J. P. Jung, J. H. Collier, *Proc. Natl. Acad. Sci. U. S. A.* **2010**, 107, 622.
- [25] I. V. Korendovych, Y. H. Kim, A. H. Ryan, J. D. Lear, W. F. DeGrado, S. J. Shandler, *Org. Lett.* **2010**, 12, 5142.
- [26] J. Boekhoven, S. I. Stupp, *Adv. Mater.* **2014**, 26, 1642.
- [27] M. C. Branco, D. M. Sigano, J. P. Schneider, *Curr. Opin. Chem. Biol.* **2011**, 15, 427.
- [28] H. Shigemitsu, I. Hamachi, *Acc. Chem. Res.* **2017**, 50, 740.
- [29] A. G. Cheetham, R. W. Chakraborty, W. Ma, H. G. Cui, *Chem. Soc. Rev.* **2017**, 46, 6638.
- [30] B. Seamonds, N. Yang, K. Anderson, B. Whitaker, L. M. Shaw, J. R. Bollinger, *Urology* **1986**, 28, 472.
- [31] S. Dedorson, A. Fritjofsson, B. J. Norlen, G. Ronquist, *Upsala J. Med. Sci.* **1983**, 88, 127.
- [32] Z. Q. Q. Feng, H. M. Wang, X. Y. Chen, B. Xu, *J. Am. Chem. Soc.* **2017**, 139, 15377.
- [33] R. Garciaarenas, F. F. Lin, D. L. Lin, L. P. Jin, C. C. Y. Shih, C. S. Chang, M. F. Lin, *Mol. Cell. Endocrinol.* **1995**, 111, 29.
- [34] S. Korenchuk, J. E. Lehr, L. McLean, Y. G. Lee, S. Whitney, R. Vessella, D. L. Lin, K. J. Pienta, *In Vivo* **2001**, 15, 163.
- [35] B. A. Roecklein, B. Torokstorb, *Blood* **1995**, 85, 997.

SUPPORTING INFORMATION

Additional supporting information may be found online in the Supporting Information section at the end of this article.

How to cite this article: Feng Z, Wang H, Yi M, et al.

Instructed-assembly of small peptides inhibits drug-resistant prostate cancer cells. *Peptide Science*. 2020;112:e24123.

<https://doi.org/10.1002/pep2.24123>